Brazability of Aluminum using Al-Si Filler Alloys with Different Compositions and Microstructures†

Ikuo OKAMOTO* and Tadashi TAKEMOTO**

Abstract

Brazability of aluminum T-joint (AA 1100) was evaluated by a fillet formation test in a vacuum using Al-Si alloys with different compositions and microstructures. The crosssection fillet leg length rotio L_V/L_H (L_V: vertical leg length, L_H: horizontal leg length) was used for evaluating the brazability, where the ratio approached unity under a good brazing condition. In filler alloys with 5 ~ 10%Si, a sound fillet could be achieved under liquidus temperature. L_V/L_H reached a plateau beyond this temperature by isothermal solidification which started at a fillet edge. Filler alloys containing fine silicon particles were preferable to ensure successful fillet shape. Iron up to 1.4% in Al-10%Si filler alloy had no influence on brazability.

KEY WORDS: (Brazing) (Brazing Fillers) (Aluminum Alloys) (Microstructure) (Composition)

1. Introduction

Vacuum brazing of aluminum has been particularly succeeded by the addition of magnesium to Al-Si filler alloys. Precise reports have been published on the brazability of brazing sheets with Al-Si-Mg alloy cladding for vacuum brazing. The works investigated the relation between the vacuum brazability of aluminum and silicon contents, magnesium contents, additional elements to filler alloy[1),2)] and vacuum level[3)]. On the other hand, fluxless brazing of aluminum is possible by using Al-Si system filler alloys without magnesium under the condition of appropriate surface pretreatment or addition of certain elements to filler alloy[4)~6)]. Material characteristics as well as processing conditions are important in brazing, however, effect of metallurgical factors on brazability have not yet been investigated precisely even Al-Si alloys have long been used for aluminum brazing.

Iron, one of the inevitable impurity elements of aluminum, forms intermetallic compounds by the addition beyond solubility limit[7)]. Iron content in filler alloy was defined under 0.8% in the JIS specification Z 3263, however, the standardized value did not seem to be well-grounded. In addition, there was an aspect that the addition of 0.2 ~ 1.2% iron might be effective to control the flow and to narrow the melting temperature range of Al-Si-Mg alloys[8)]. Magnesium in filler alloy as well as iron also might affect the flow and melting temperature range. Consequently the effect of iron content in filler alloy, especially in Al-Si alloys, on brazability must be examined clearly.

Aluminum surfaces are generally covered with self-healing and protective oxide films that act as barriers to flow, wetting and fillet formation during brazing. Since Al-Si alloy used in this work has no getter elements such as magnesium, surface oxide film seems to give considerable effect on brazability. The present investigation was performed to determine the effect of composition, iron content, silicon particle size and surface oxide film of filler alloys on brazability of aluminum.

2. Experimental Procedures

Commercially pure aluminum (**AA 1100**, 0.23%Fe, 0.08%Si) was used as a base material. The composition of filler alloys employed in the present work are shown in **Table 1**. Five commercial filler alloys and four laboratory made ones were used. Laboratory alloys were made from 99.99% aluminum, 99.999% silicon and high purity Al-Fe alloy. The cast alloys were fabricated by hot extrusion to rods of 2.4 mm diameter and subsequently cold rolled to 1.35 mm thickness. Commercial filler alloys of 2.4 mm diameter were also cold rolled to 1.35 mm thickness.

† Received on October 9, 1981
* Professor
** Research Instructor

Transactions of JWRI is published by Welding Research Institute of Osaka University, Suita, Osaka, Japan

Table 1 Chemical composition of filler alloys.

Filler alloys	Elements								
	Si	Fe	Cu	Mn	Mg	Cr	Ti	Zn	Al
4043	4.96	0.15	tr.	tr.	tr.	tr.	tr.	tr.	bal.
4343	7.66	0.10	0.02	tr.	tr.	tr.	tr.	tr.	bal.
4045	9.73	0.13	tr.	tr.	tr.	tr.	tr.	tr.	bal.
4047	12.1	0.34	tr.	tr.	tr.	tr.	tr.	tr.	bal.
4145	9.58	0.40	3.99	0.02	0.05	tr.	0.02	0.05	bal.
A	10.32	tr.	tr.	tr.	tr.	tr.	tr.	tr.	bal.
B-1	10.98	0.13	tr.	tr.	tr.	tr.	tr.	tr.	bal.
B-2	9.90	0.46	tr.	tr.	tr.	tr.	tr.	tr.	bal.
B-3	10.10	1.36	tr.	tr.	tr.	tr.	tr.	tr.	bal.

tr. <0.01

Brazability was evaluated by making fillet joints in an inverted "T" configuration which was composed of vertical and horizontal members ($12^h \times 25^l \times 3^t$, $25^w \times 35^l \times 3^t$, in mm respectively) of **1100** aluminum. Both members (base plates) were polished by 600 grade emery paper prior to brazing. Filler alloy of 25 mm length was set between vertical and horizontal members and a load of about 20 g/mm^2 was applied by a heat resistant spring. Speciments were heated in a vacuum furance at temperatures ranging from about 570 ~ 635°C. Vacuum level was about 2×10^{-5} torr.

Brazed specimens were cut at center and polished for measurement of brazing parameters and metallographic examination. Fillet leg length ratio (L_V/L_H, L_V: vertical leg length, L_H: horizontal leg length), crosssectional fillet area (S_F), and eroded area (S_e) were used to reveal joint formation characteristics of filler alloys under various test temperatures (**Fig. 1**). The values of S_F and S_e were the sum of fillet area of both sides. The measurement of silicon particle size were made along rolling direction (D_H) and at right angles to this direction (D_T) respectively. About 300 particles were measured using the profile projector by measuring the length of silicon particles on mesh of 50 μ distance drawn in micrographs of magnification of 340. Precise experimental techniques were shown in the previous papers[9), 10)].

3. Results and Discussions

3.1. Effect of silicon content

Brazability was evaluated by the measurement of fillet leg length ratio, L_V/L_H, which indicated the fillet formability on the joint and the value approached unity under good brazing condition. The effects of filler alloy composition on L_V/L_H at various brazing temperatures are shown in **Fig. 2**. Over the temperature range investigated, L_V/L_H in each filler alloy reached a plateau at certain temperature, where the valus of L_V/L_H exceeded 0.8. The temperatures that L_V/L_H reached plateaus were 615°C for 4043 filler alloy, 590°C for 4343, 4045 and 4047 filler alloys and 580°C for 4145 filler alloy. Above

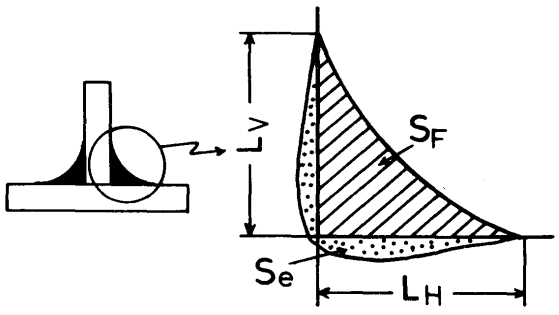

Fig. 1 Schematic symboles of crosssectional fillet, S_F: fillet area, S_e: eroded area, L_V: vertical leg length, L_H: horizontal leg length.

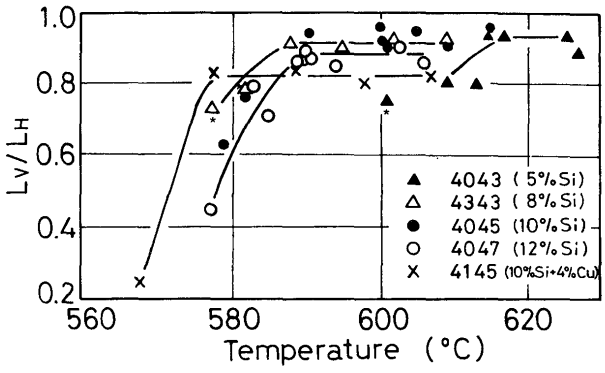

Fig. 2 Changes of L_V/L_H with brazing temperatures.

these temperatures, smooth fillet surface without roughening due to microschrincage and excellent fillet shape by uniform flow were obtained. The mark * in Fig. 2 indicates the convex fillet surface due to the relatively low brazing temperature, of course under liquidus, indicating it was so low that partialy melted filler alloy could not flow sufficiently to form concave surface.

Fillet area (S_F) and eroded area (S_e) are shown in **Fig. 3**. Fillet areas of Al-5 ~ 8%Si filler alloys were smaller than that of filler alloys with 10 ~ 12%Si, and moreover the temperature dependences of S_F and S_e were also smaller in the former filler alloys than the latters. Scattering of data in S_F was larger than L_V/L_H as already mentioned in previous paper[10]. Eroded area increased with silicon content, rise in brazing temperature and addition of copper to filler alloy. Woods *et al*[11] investigated the flow factor and diffusion of silicon to base metal in dip brazing process using brazing sheets. The report described that the change of the brazing temperature of 6°F corresponded the change of 1% silicon content in brazing sheet cladding. In the present work, from the relation between temperature and silicon content with reference to the same value of eroded area shown in Fig. 3, the change of silicon content of 1% corresponded the change of brazing temperature of 4°C, which gave good agreement with the result of Woods *et al.*[11].

Figure 4 shows the residual filler alloy thickness between vertical and horizontal members. Residual thickness decreased with increasing silicon content and brazing temperature. Residual thickness of 4145 filler alloy is thinner than that of 4045 filler alloy with even silicon content. As the solidus temperature of 4145 filler alloy is about 57°C lower than that of 4045 filler alloy, the amount of liquid is greater in former alloy than the latter at relatively low temperatures. The amount of residual filler alloy can be determined from Fig. 4, then the theoretical fillet area (S_{FT}) can be calculated from the equation, (used amount) – (residue) = (fillet). **Figure 5** represents the ratio of observed fillet area (S_{FO}) to theoretical one (S_{ST}), S_{FO}/S_{FT}. As shown in the figure, the value of S_{FO}/S_{FT} of 4343 filler alloy was quite near to the calculated one and was also nearly equal to unity in 4043 filler alloy. In the other alloys the value exceeded unity, especially at higher temperatures the fillet size at longitudinal center of specimen is extremely larger than theoretical one. **Figure 6** exhibits the distribution of fillet area along longitudinal direction of tee joint brazed with 4047 and 4343 filler alloys. Uniform filler alloy flow was obtained in alloys with less silicon content (5~8%), however, fillet at center became large in alloys with much

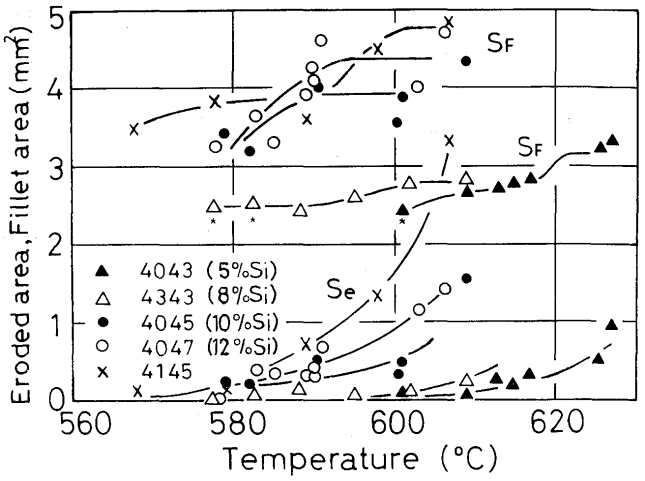

Fig. 3 Changes of fillet area and eroded area with brazing temperatures.

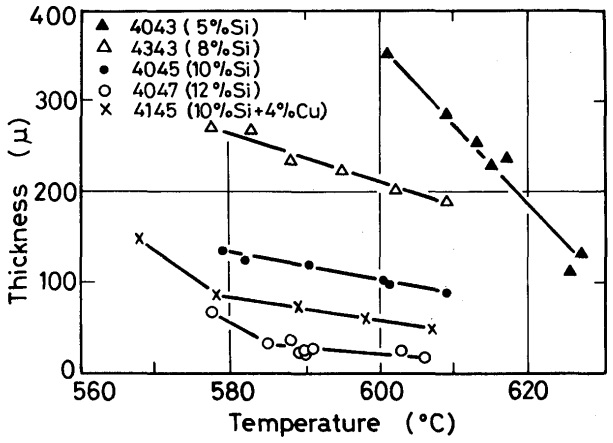

Fig. 4 Residual thickness of filler alloy between vertical and horizontal members brazed with various filler alloys.

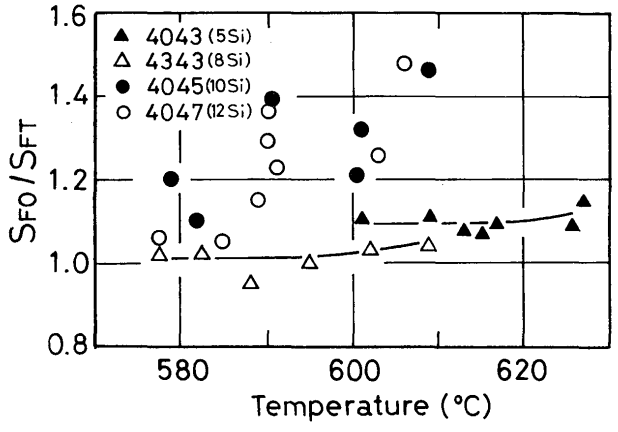

Fig. 5 S_{FO}/S_{FT} of various filler alloys.

silicon content (10 ~ 12%). One of the reason that the fillet area becomes small at edge of specimen may be edge effect[13]. As will be mentioned in the following section, solid phase in liquid divided the meniscus (concave surface formed by the molten filler alloy at fillet) under liquidus temperature, consequently the edge effect in less silicon content alloys was decreased. Recently Kawakatsu *et al.*[14] investigated the effect of bismuth addition to Al-10%Si-1%Mg filler alloy. The work demonstrated that the uniform distribution of fillet size was obtained by addition of 0.1%Bi to Al-10%Si-1%Mg cladding of brazing sheets. The distribution of fillet size may be dependent on viscosity, surface tention of molten filler alloy and other physical properties, however, precise effect and mechanisms are not clear.

The solid lines in **Fig. 7** indicate the theoretical ratio of liquid phase* for alloys with different silicon content. The broken lines in Fig. 7 represent the observed liquid phase ratio under the hypothesis that the whole residue between vertical and horizontal members indicated in Fig. 4 was solid phase and the portion which contributed fillet formation was liquid**. The broken lines intersected the solid ones at certain temperatures except 12.1%Si filler alloy. The cross temperature almost corresponds the temperature where L_V/L_H reached a plateau shown in Fig. 2. Under the cross temperature, the amount of solid phase between vertical and horizontal members was lesser than the equilibrium one. The applied load may extruded the solid phase and it contributed the fillet formation. In fact, a few specimens showed a convex surface fillet appearance. Above the cross temperature, the amount of solid phase is more than the equilibruim one. In the intereior of clearance, new α-Al phase crystalized from the coexisting liquid by diffusion of silicon into base plate. Accordingly, during holding at brazing temperature, isothermal solidification process proceeded. From the above mentioned discussion, within the lower temperature range than the cross temperature, solid phase is extruded during heating stage to form fillet and then it liquefied with the rise in temperature. Above the cross temprature isothermal solidification took place as already mentioned. Since both tips of the fillet at vertical and horizontal members are easily affected by isothermal solidification in comparison with central part of fillet, L_V/L_H and S_F almost constant above the cross temperature. In 12.1%Si filler alloy, the observed line did not intersect the theoretical one, and the amount of liquid phase is lesser than the equilibrium one. Whole constituent becomes almost liquid above the eutectic temperature, therefore, the base plate dissolved into filler alloy and then the solid phase will be crystalized from liquid by diffusion of silicon into base plate.

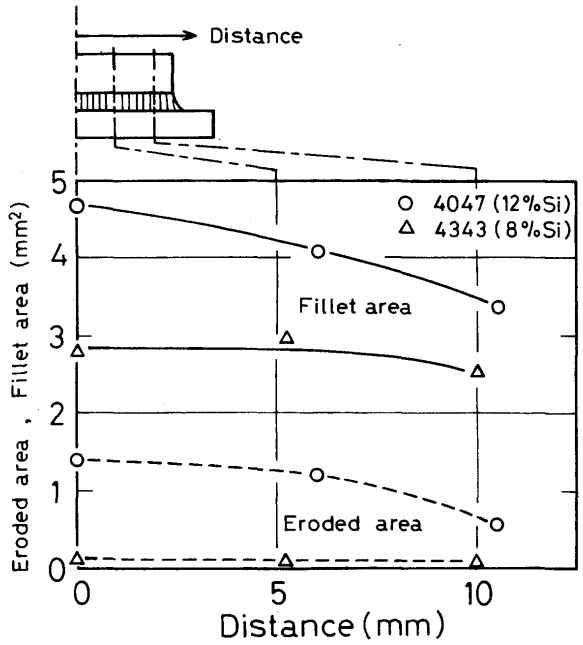

Fig. 6 Variation of fillet area and eroded area in brazed tee joint from center to edge.

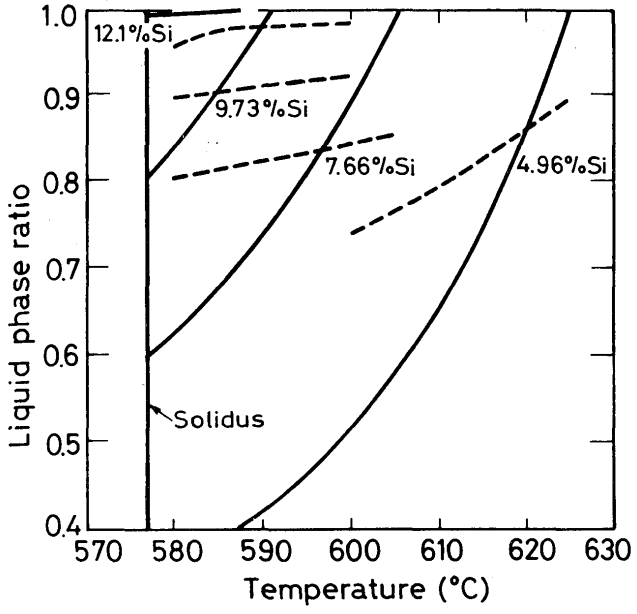

Fig. 7 Calculated liquid phase ratios (solid lines) and observed ones (dotted lines) for various filler alloys as a function of temperature.

* The theoretical lines were drawn under hypothesis that the liquidus and soludus in Al-Si binary equilibrium diagram were straight lines.

** Generally, the solid phase is extruded from clearance and also molten liquid is confined within the clearance during brazing heat cycle.

Table 2 Changes of silicon particle size in 4045 filler alloy by vacuum annealing.

4045 filler alloy	Treatment	Si particle size (μ)		D_H/D_T	$(D_H+D_T)/2$
		D_H	D_T		
(a)	As cold rolled	4.1	2.6	1.57	3.35
(b)	Annealed at 565 °C for 4 h	6.2	4.7	1.34	5.45
(c)	Annealed at 572 °C for 8h	15.3	13.0	1.18	14.1

3.2. Effect of microstructure of filler alloy

Scharples[16] investigated the effect of grain size of brazing sheet claddings on flowability. They reported that coarse α-Al grain interrupted flow of eutectic liquid and caused decrement in flow factor. Woods[17] reported that flow factor was increased by the decrease in silicon particle size of claddings. It is clear that filler alloys with fine microstructure can easily liquefy. The present work dealt with the effect of silicon size on fillet formation in preplaced brazing method. Silicon particle size was changed by annealing of 4045 filler alloy in vacuum. **Table 2** shows the mean value of silicon particle size after each treatment. The silicon particles grew and became round by annealing, consequently the value of D_H/D_T decreased showing small rolling direction dependence. **Figure 8** shows the relation between brazability (L_V/L_H) and silicon particle size, which is indicated by a parameter, $(D_H+D_T)/2$. Brazability (L_V/L_H) decreased with the increase in particle size, accordingly it is clear that the fine microstructure is superior in brazability. Alloys with 14.1 μ particle size showed remarkably uniform fillet shape at 600°C brazing. Moreover, L_V/L_H was less than 0.7 even at higher brazing temperature. From Fig. 8, the coarsening in silicon particle resulted in the degradation of brazability. The apparent melting point of alloy with coarse silicon particle, at heating stage during brazing, is 4°C higher than that of the alloy with fine structure. The difference in the apparent melting point is caused by the difference in time for liquefy. Since the alloys with coarse silicon particle have less α-Al/silicon interface in comparison with fine ones, much time is required for complete liquefying by eutetic reaction. As braze specimen was rapidly heated, the melting point increased apparently. For this reason, the alloys with coarse silicon particle filler alloy began to flow at relatively higher temperature than solidus temperature even it was heated to the temperature range where L_V/L_H was constant at indicated in Fig. 2, and thereby the molten alloy spread on horizontal members[10].

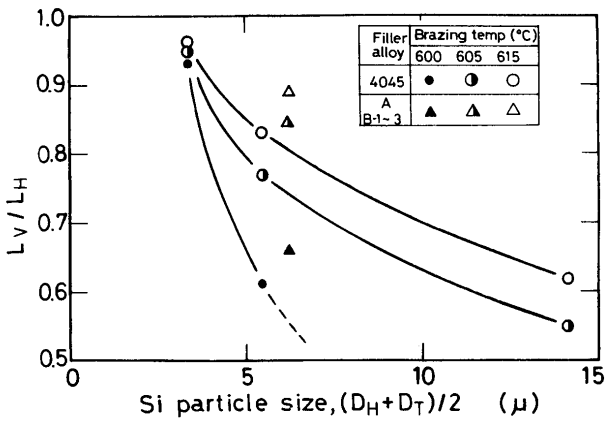

Fig. 8 Effect of silicon particle size in filler alloy on brazability.

3.3 Effect of iron content in filler alloys

Figure 9 shows the microsturcture of cold rolled laboratory made filler alloys. The silicon particle size of laboratory made filler alloys are larger than that of commercial 4045 filler alloy **(Fig. 10)**, however any significant differences were noted in microstructure and silicon particle size of the four materials with different iron contents. The mean value of silicon particle sizes of A,B-1 ~ 3 filler alloys are as follows: $D_H = 8.0\,\mu$, $D_T = 4.3\,\mu$, $D_H/D_T = 1.83$, $(D_H+D_T)/2 = 6.15\,\mu$. **Table 3** shows the brazability of filler alloys with different iron content (0 ~ 1.36%Fe). As shown in the table, the difference in brazability (L_V/L_H) based on the iron content was not observed. The appearances of specimens brazed with A and B-3 alloys are shown in **Fig. 11**. The B-1 ~ 3 alloys with iron showed rather rough surface and the alloy A showed somewhat wrinkled surface. Rough surface was seemed to be caused by the microschrincage during solidification. Therefore, the smoothness of surface may be dependent on the content of gaseous component and silicon particle size. Hayashi *et al.*[18] investigated the cause of microschrincage on fillet surface and concluded that microschrincage was apt to form if calcium content in Al-Si-Mg filler alloys exceeded a certain level. The relation between the results of this work and their reports and also the precise mechanism of the formation of

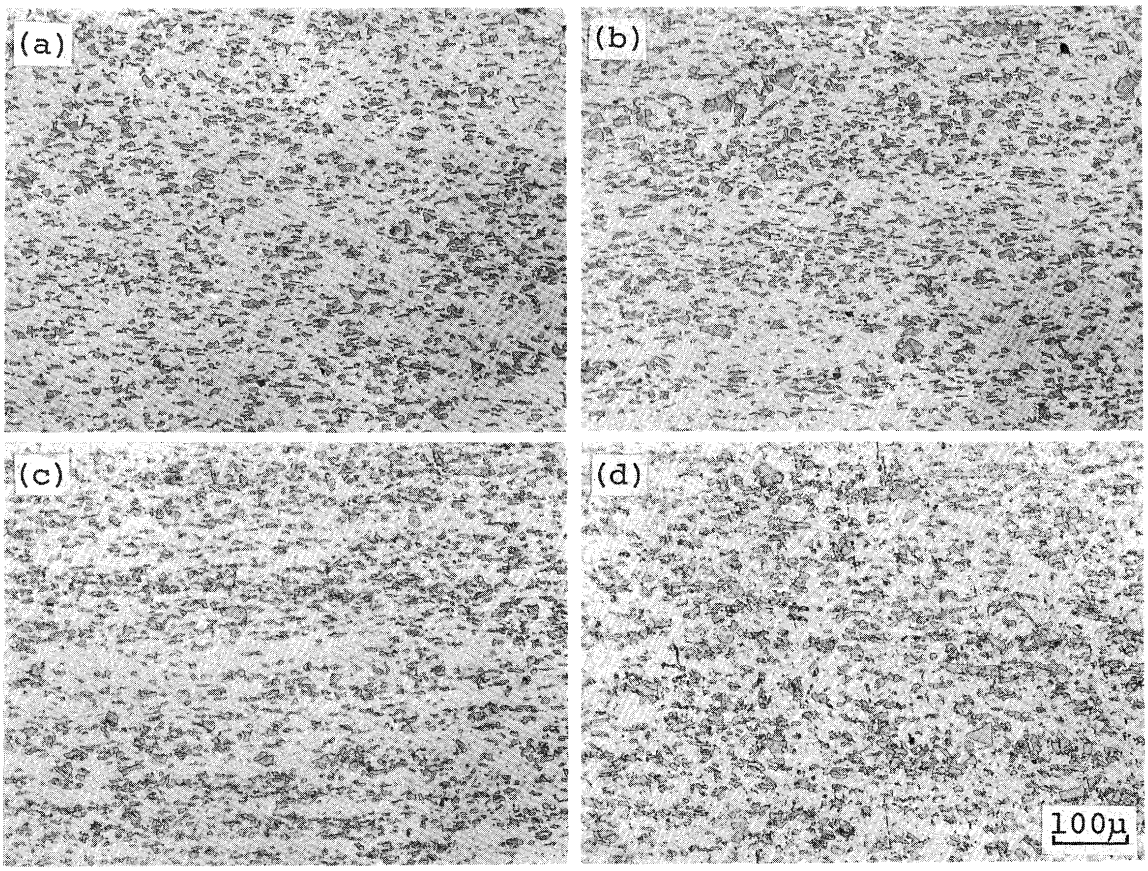

Fig. 9 Micrographs of laboratory made Al-10%Si filler alloys A(0%Fe) (a), B-1(0.13%Fe) (b), B-2(0.46%Fe) (c) and B-3(1.36%Fe) (d).

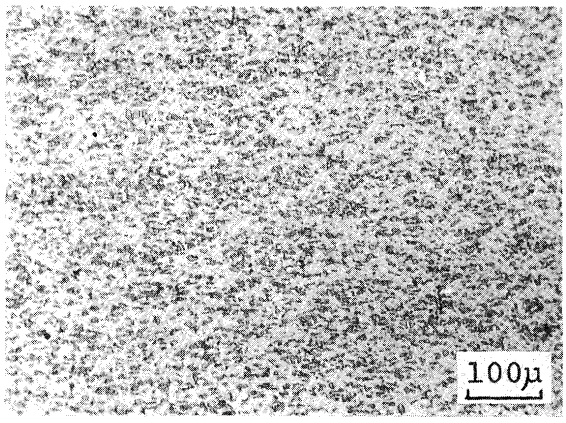

Fig. 10 Micrographs of commercial 4045 filler alloy.

Table 3 Relation between iron content in Al-10%Si filler alloys and L_V/L_H after brazing at 600 ~615°C.

Filler alloys	Brazing temperatures (°C)		
	600	605	615
A (0%Fe)	0.67	0.84	0.89
B-1 (0.13%Fe)	0.63	0.79	0.88
B-2 (0.46%Fe)	0.65	0.87	0.88
B-3 (1.36%Fe)	0.69	0.88	0.92

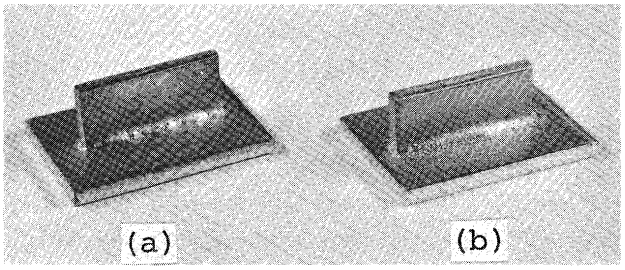

Fig. 11 Appearance of fillet brazed with alloy A (a) and alloy B-3 (b).

mocroschrincage and wrinkle were not clear enough. The relation between mean value of L_V/L_H and $(D_H + D_T)/2$ for laboratory made filler alloys at various temperatures was shown in Fig. 8 by triangles. The values of L_V/L_H were higher than the annealed commercial 4045 filler alloy at same silicon particle size. Since laboratory made alloys were in as cold rolled condition, the silicon particle has cracks, rather coarse irregularities and moreover the high lattice defects density. On the other hand, the silicon particle in annealed 4045 alloy with same size was rather round, as D_H/D_T approached unity after annealing.

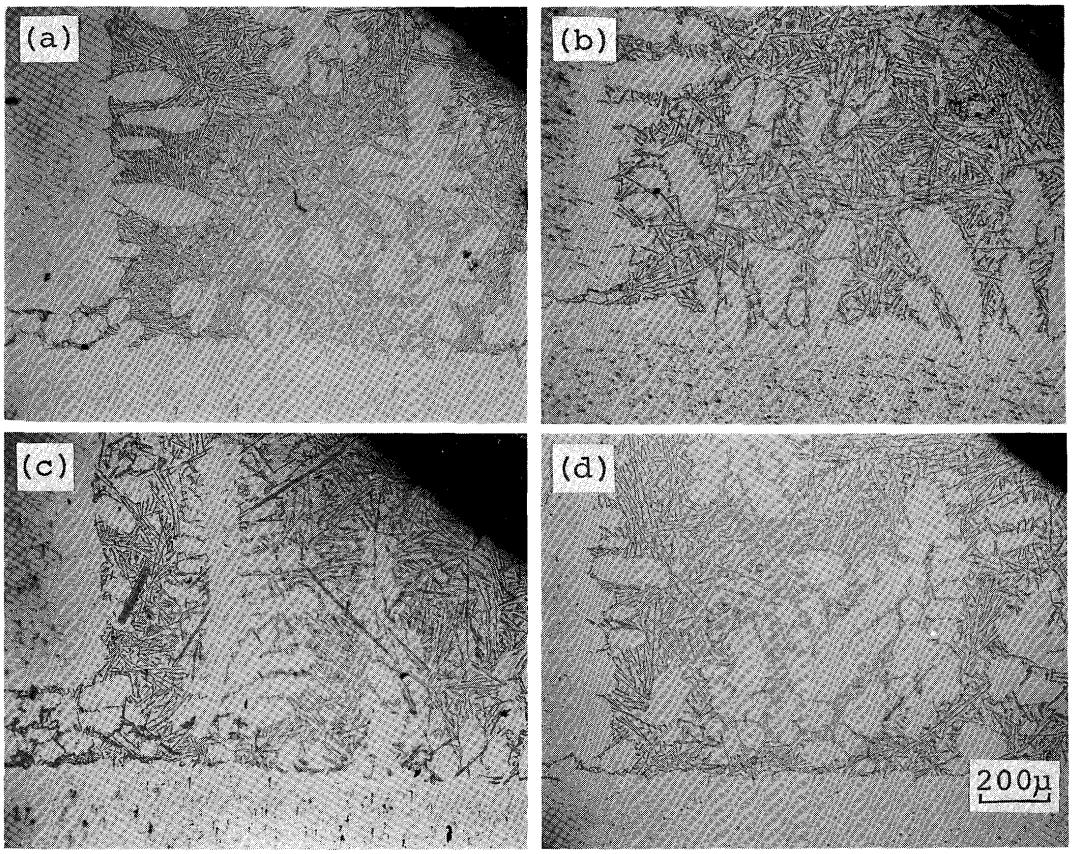

Fig. 12 Micrographs of fillet brazed using Al-10%Si filler alloys with various iron contents, A (0%Fe) (a), B-2(0.13%Fe) (b), B-3 (1.36%Fe) (c) and 4045 (0.13%Fe) (d).

Therefore even same silicon particle size, cold rolled alloys has larger silicon/α-Al interface area than that of annealed one.

Figure 12 presents the microstructure of fillet brazed at 605°C. Fine eutectic structure is shown in alloy A without iron, and the eutectic structure became a little coarse by addition of iron. The alloy with 1.36%Fe exhibited large acicular Al-Si-Fe intermetallic compound. Furthermore large square silicon particles were observed in B-1 ~ 3 alloys compared with commercial 4045 alloy.

The results indicated that the iron up to 1.36% in Al-10%Si alloys did not give a remarkable influence on brazability, however, solidified fillet microstructure is something different. Bestumiya *et al.*[19] studied the relation between mechanical properties of Al-Si cast alloys and iron content. The paper described that Al-Si-Fe system intermetallic compound was observed in alloys with more than 0.4%Fe and the formation of compound resulted in low toughness. Komiyama *et al.*[20] also demonstrated that the addition of more than 0.5%Fe drastically reduced elongation. From these works, the standard value in JIS specification Z 3263 (< 0.8%) is believed to admits of some arguments under consideration of its mechanical properties, however, from the point of view of brazing there is no problem as brazability was not influenced by the iron content of filler alloy. In addition to this, the use of high purity Al-Si alloy by progressive refinement has no significance with respect to brazing characteristics.

3.4. Effect of surface oxide film of filler alloy

Figure 13 exhibits the distribution of fillet area and L_V/L_H using 4047 filler alloy with 1.35 mm thickness and 12.5 mm length. The alloy was inserted at center of specimen, where fillet area and L_V/L_H is small. Between the edge and preplaced position, almost ideal fillet, that L_V/L_H was unity, was formed. At the preplaced position, the preexisted surface oxide seems to be still remained even though it was broken and dispersed on fillet surface during extrusion from the clearance between vertical and horizontal members after melting, and it slightly decreased L_V/L_H. One of the reason of the success of the insert type brazing with Al-Si filler alloy was that the applied load on vertical member pushed down it when the alloy melted, and this displacement destroyed the oxide film on filler alloy to the extent that sound fillet formation could

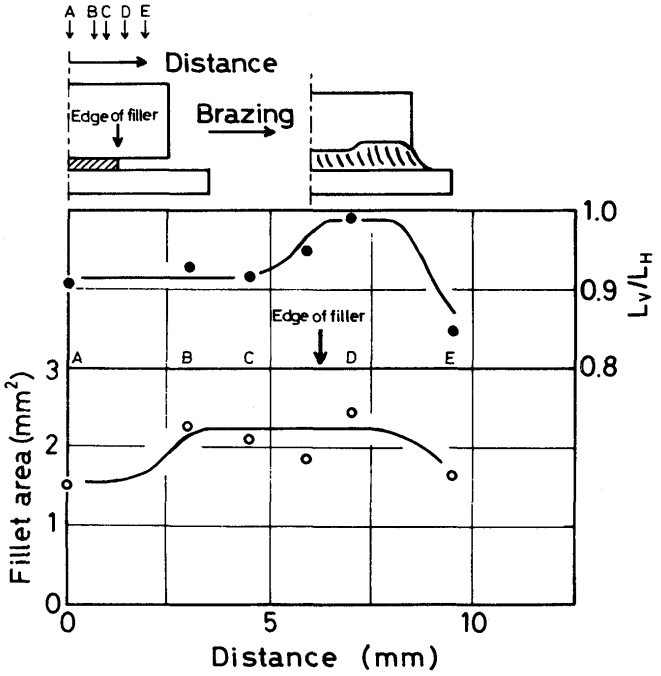

Fig. 13 Distribution of fillet size and L_V/L_H brazed with 4047 filler alloy of 12.5 mm length and 1.35 mm thickness.

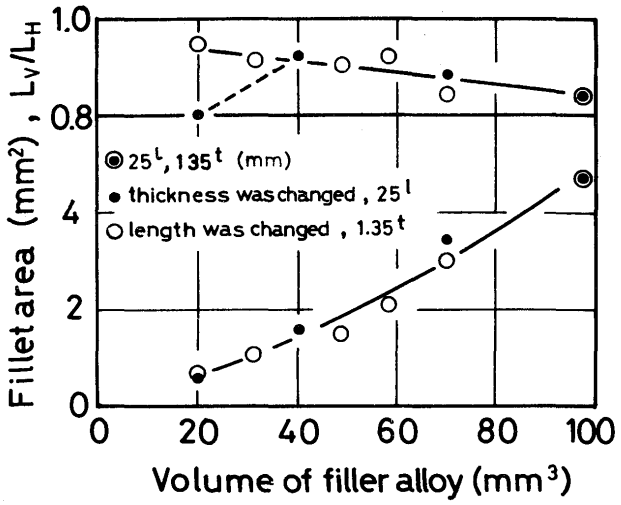

Fig. 14 Effect of filler alloy thickness and volume on L_V/L_H and fillet area.

be achieved.[10] As extruded liquid was relatively free form continuous oxide film, it provided the uniform flow, quick wetting and sound fillet formation. Then change of initial distance between vertical and horizontal members, *i.e.* filler alloy thickness will also affect brazability because the degree of surface film destruction will be varied by the difference in extruded amount. **Figure 14** shows the effect of volume of filler alloy on L_V/L_H. The volume was changed by two ways, one was thickness and another was length, the results were indicated by solid and open circles respectively. Fillet area increased with increasing the volume of filler alloy, whereas L_V/L_H slightly decreased with the increase of volume. As increased volume of fillet provides large L_V, gravitational effects may be a factor in decreasing L_V/L_H. L_V/L_H showed slight dependence on the volume of filler alloy irrespective of the change in thickness and length, except the volume of 20 mm^3. At this volume, L_V/L_H indicated by solid circle was obtained by using the alloy with 0.25 mm thickness. Only this value was slightly lower than the open circle using the alloy with 1.35 mm thickness. Under the brazing conditon of the present work, initial clearance of more than 0.5 mm seems to be preferable to break down the surface oxide film sufficiently.

4. Conclusions

The effects of filler alloy composition, microstructure and iron content on brazability were investigated using Al-10%Si filler alloys and 1100 aluminum base plate. Obtained results were summarized as follows.

(1) The lowest temperatures to permit sound fillet formation were 615°C for 5%Si alloy, 590°C for 8 ~ 12%Si alloys, and 580°C for 10%Si + 4%Cu filler alloys.

(2) The lowest temperatures to permit sound fillet formation was located under the liquidus temperature, and above this temperature L_V/L_H reached a plateau by the isothermal solidification which started at tips of fillet on vertical and horizontal members.

(3) Filler alloys with coarse silicon particle showed poor brazability, consequently silicon particle refinement is perferable to insure good brazability.

(4) Iron content in filler alloys up to 1.4% had no influence on brazability, however, lesser amount than standard value (< 0.8%) seemed to be preferable under consideration of its mechanical properties.

(5) Surface oxide on filler alloys slightly decreased the value of L_V/L_H even the oxide seemed to be broken during extrusion from preplaced position between vertical and horizontal members.

The authors are very much appriciated to Prof. Dr. Shigenori Hori and Dr. Norio Furushiro at Faculty of Engineering of Osaka University, Dr. Yoshihiko Sugiyama and Mr. Hiroshi Irie of Sumitomo Light Metal Industries Ltd. for preparing specimens and chemical analysis. Thanks are also to Mr. Kei Uchikawa at Ajikawa Iron Works & Construction Co., Ltd. for experimental works.

References

1) H. Kawase, M. Yamaguchi and K. Tanaka: J. Light Metal Weld. Construction. **11** (1973), 115.
2) H. Kawase, M. Yamaguchi: *ibid.*, **15** (1977), 345.
3) H. Yoshida and Y. Takeuchi: J. Japan Inst. Light metals, **27** (1977), 121.
4) M.M. Schwarz, F.B. Gurtner and P.K. Shutt, Jr.: Weld. J., **46** (1967), 423.
5) C.S. Beuyukian: Weld. J., **47** (1968), 710.
6) H. Schöer and W. Schultze: Z. Metallkde, **63** (1972), 775.
7) For example, H. Watanabe and E. Sato: *Explanatory Equilibium Diagram for Commercial Alloys*, (1966), Nikkan-kogyo.
8) Patent: S 53-15974
9) I. Okamoto and T. Takemoto: Trans. JWRI, **6** (1977), 139.
10) I. Okamoto and T. Takemoto: Trans. JWRI, **7** (1978), 135.
11) R.A. Woods and I.B. Robinson: Weld. J., **53** (1974), 440s.
12) JIS Z 3263
13) H. Peth: J. mater. Tech., **11** (1975), 367.
14) I. Kawakatsu and T. Osawa: J. Light Metal Weld. Construction, **18** (1980), 101.
15) M. Hansen: *Constitution of Binary Alloys*, (1958), McGrawhill Book Co., 132.
16) P. Sharples: Weld. J., **54** (1975), 164.
17) R. A. Woods: Aluminium, **54** (1978), 444.
18) Y. Hayashi, S. Takeno, T. Yoneyama: Preprints of National Meeting of J.W.S., No. 25 (1979), 118.
19) N. Beck and O. Ueda: J. Japan Inst. Light Metals, **27** (1977), 189.
20) Y. Komiyama, K. Uchida and M. Gunshi: *ibid.*, **26** (1976), 311.